Supplementary Material

EXPERIMENTAL PROCEDURES

NMR Spectroscopy--NMR spectra were acquired at 37°C on 750- and 500-MHz Varian NMR spectrometers with self-shielded z-axis gradients. All spectra were processed using NMRPipe (1, 2) and analyzed using SPARKY 3 (Goddard and Kneller, University of California, San Francisco). The ^{1}H,^{15}N, and ^{13}C resonances of the protein backbone and side chain atoms were assigned by using a standard set of triple resonance experiments on a uniformly ^{15}N,^{13}C-labeled CBD (concentration ~0.6mM) (3-5). The initial backbone assignment was generated by MARS (6) and manually checked in combination with ^{15}N-edited 3D NOESY. Aromatic moieties were obtained by $(H_\beta)C_\beta(C_\gamma C_\delta)H_\delta$, $(H_\beta)C_\beta(C_\gamma C_\delta C_\varepsilon)H_\varepsilon$ (7). NOE-derived distance restraints were obtained from ^{15}N- or ^{13}C-edited 3D NOESY spectra, complemented by a 2D H, H-NOESY, each with a mixing time of 150 ms. Residual dipolar couplings were obtained by using the IPAP-type ^{15}N-HSQC experiments (8). Structurally predicted RDCs were calculated using the program PALES (9). $\{^{1}H\}$-^{15}N-NOE and Sea-HSQC (10) with a mixing time of 100 ms were applied in the 500-MHz spectrometer.

NOE Analysis and Structure Calculations--NOE assignment and structure calculations were performed using the CANDID (11) module of the program CYANA2.1 (12). Unassigned resonances that were unambiguously involved in NOE contacts were represented by appropriate proxy residues (13) during the structure calculations. The final set of NOE restraints together with H-bond restraints and dihedral restraints from TALOS (14) was recalculated and used to carry out a water refinement in CNS (15) following the standard RECOORD protocol (16). The quality of the structures was assessed using WHATCHECK (17), PROCHECK (18) and analyzed by MOLMOL (19). The solvent accessibility was calculated by NACCESS (20). All of the figures representing the structures were generated by Pymol (http://www.pymol.org).

Binding studies--To investigate the ligand binding, the 2D ^{1}H-^{15}N-HSQC spectra were recorded on uniformly ^{15}N-labeled CBD (~0.2mM) in the presence of different concentrations of MBD ranging from 0 to 1.5 mM. Both the CBD sample and the stock solutions of MBD were prepared in the NMR buffer (50 mM sodium phosphate, 50 mM NaCl, 5% glycerol, and 1 mM EDTA, pH 7.5). The chemical shift perturbation between the free-form and MBD-bound CBD was normalized by the following formula and expressed in ppm:

$$\text{Chemical shift perturbation} = \sqrt{(\Delta\delta H)^2 + (\frac{\Delta\delta N}{6})^2},$$

where $\Delta\delta H$ and $\Delta\delta N$ are the differences in chemical shifts of amide protons and nitrogen between the initial and final data points of the titration, respectively.

Yeast two-hybrid assay--To identify interaction domains of Mcm6 and Cdt1, a yeast two-hybrid assay was performed with the Matchmaker Gal4 two-hybrid system 3 (Clontech). The cDNA encoding the full-length or various fragments of Mcm6 were cloned into the bait vector pGBKT7. The full-length or fragments of Cdt1 cDNA were cloned into the prey vector, pGADT7. The assay was conducted according to the manufacturer's instructions.

Site-directed mutagenesis--Expression constructs for Mcm6 mutants were generated with the QuickChange kit (Stratagene). The presence of appropriate mutations was confirmed by DNA sequencing.

Table S1. Statistics of the NMR structure of Mcm6 CBD

(a) NMR restraints		
Total Experimental Restraints		*1513*
Total NOE Distance Restraints		*1355*
Short-range, |i-j|<=1		*775*
Medium-range, 1<|i-j|<5		*343*
Long-range, |i-j|>=5		*237*
Hydrogen bonds		*30*
Dihedral restraints		*128*
(b) Statistics for structures		
Final Energies (kcal/mol)		
Total	*(kcal/mol)*	*-4234.90 ± 343.12*
Bonds	*(kcal/mol)*	*47.4228 ± 5.5965*
Angles	*(kcal/mol)*	*181.279 ± 27.118*
Improper	*(kcal/mol)*	*71.9450 ± 11.674*
Dihedral	*(kcal/mol)*	*572.221 ± 15.529*
van der Waals	*(kcal/mol)*	*-442.637 ± 30.904*
Electrosatatic	*(kcal/mol)*	*-4653.59 ± 323.19*
NOE	*(kcal/mol)*	*0.41880 ± 0.2026*
(c) Violations		
Number of NOE violations > 0.5Å		*0 ± 0*
R.m.s. deviation (Å) from experimental distance restraints		*0.0158 ± 0.0020*
Number of dihedral angle constraint violations > 5°		*0 ± 0*
R.m.s. deviation (°) from experimental torsion restraints		*0.2268 ± 0.0725*
(d) Deviations from idealized geometry		
Bonds (Å)		*0.01035 ± 0.0004*
Angles (°)		*1.20946 ± 0.0972*
Improper (°)		*1.48150 ± 0.0821*
(e) Structural RMSD to the mean coordinate		
region (residue number)		*bb/heavy (Å)*
708 – 821		*2.742/3.032*
718 –736,745-756,763-781,787-790,810-813		*0.531 / 1.149*
(f) WHATCHECK Structure Z-scores		
1st generation packing quality		*-1.464 ± 0.371*
2nd generation packing quality		*-2.166 ± 0.735*
Ramachandran plot appearance		*-2.910 ± 0.859*
chi-1/chi-2 rotamer normality		*-2.038 ± 0.933*
Backbone conformation		*-2.670 ± 0.878*
(g) Ramachandran plot (% residues)		
Residues in most favored regions		*81.7%*
Residues in additional allowed regions		*11.9%*
Residues in generously allowed regions		*4.60%*
Residues in disallowed regions		***1.80%***

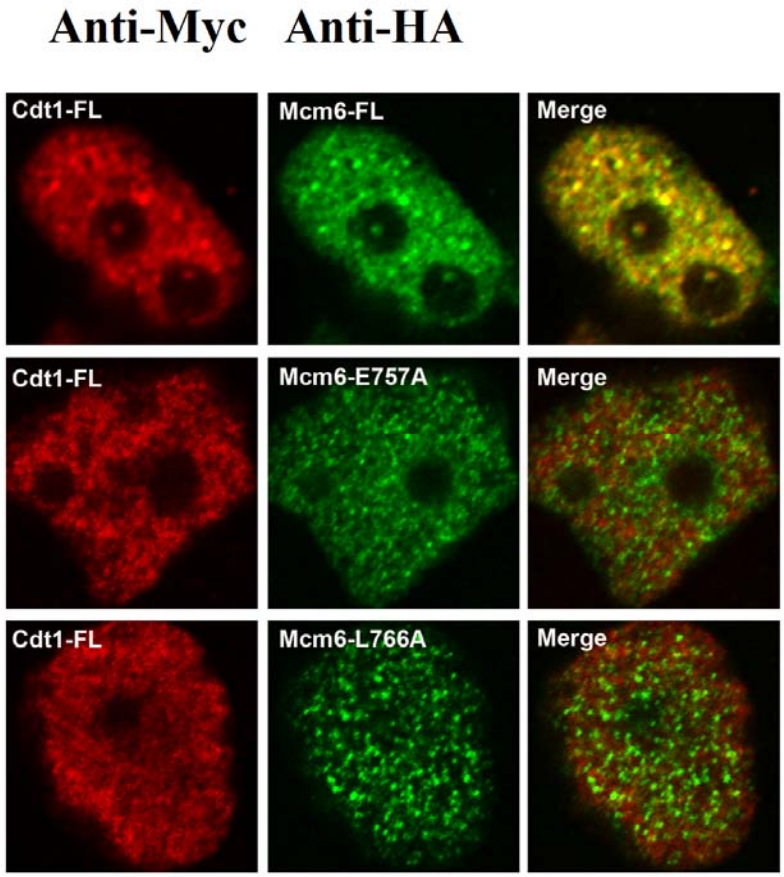

Fig. S1 The effect of a single-point mutation in the full-length Mcm6 on the *in vivo* Mcm6-Cdt1 co-localization. 293T cells co-transfected with HA-tagged Mcm6 or its mutants (green) and Myc-tagged Cdt1 (red) were immunostained using anti-HA and anti-Myc antibodies, followed by anti-rabbit IgG-Alexa 488 and anti-mouse IgG-Cy3. The images shown are extended focus views obtained by maximum projection of confocal images along the Z axis.

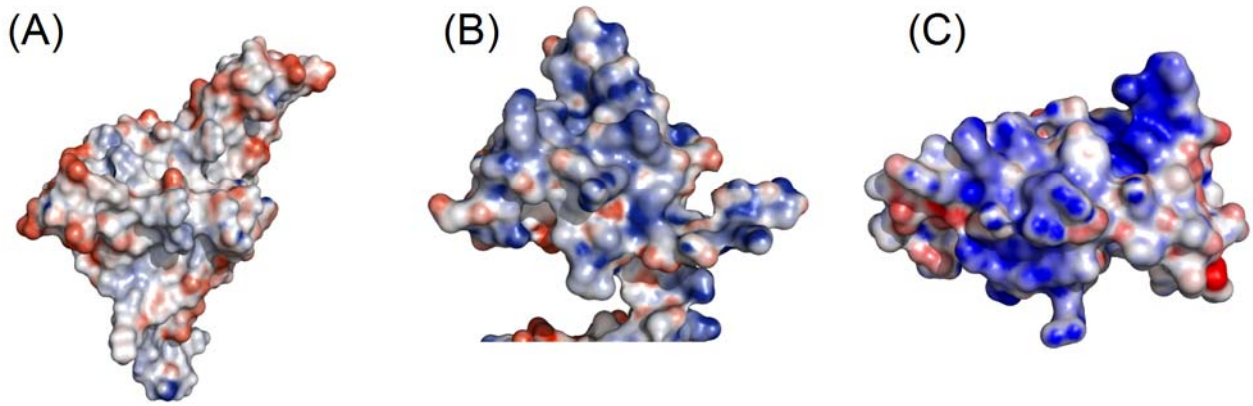

Fig. S2 The electrostatic surface potential of DNA binding proteins. (A) Mcm6-CBD, (B) Protein transcription factor E2F-4 (1CF7) and (C) Penicillinase Repressor (1XSD).

REFERENCES

1. Delaglio, F., Grzesiek, S., Vuister, G.W., Zhu, G., Pfeifer, J., & Bax, A. (1995) *J. Biomol. NMR* 6, 277-293
2. Zhu, G., and Bax, A., (1992) *J. Magn. Reson.* 100, 202-207
3. Bax, A., & Grzesiek, S. (1993) *Acc. Chem. Res.* 26, 131-138
4. Sattler, M., Schleucher, J., & Griesinger, C. (1999) *Prog. Nucl. Magn. Reson. Spectrosc.* 34, 93–158
5. Clore, G.M. & Gronenborn, A.M. (1998) *Trends in Biotechnology* 16, 22-34
6. Jung, Y.S., & Zweckstetter, M. (2004) *J. Biomol. NMR* 30, 11-23
7. Yamazaki, T., Forman-Kay, J.D., and Kay, L.E. (1993) *J. Am. Chem. Soc*. 115, 11054–11055

8. Ottiger, M., Delaglio, F., & Bax, A. (1998) *J. Magn. Reson.* 131, 373-378
9. Zweckstetter, M., and Bax, A. (2000) *J. Am. Chem. Soc.* 122, 3791-3792
10. Lin, D., Sze, K.H., Cui, Y., Zhu, G.. (2002) *J. Biomol. NMR* 23, 317-22
11. Herrmann, T., Güntert, P., & Wüthrich, K. (2002) *J. Mol. Biol*. 319, 209–227
12. Güntert, P., Mumenthaler, C., & Wüthrich, K. (1997) *J. Mol. Biol.* 273, 283–298
13. AB, E., Pugh, D. J., Kaptein, R., Boelens, R., & Bonvin, A.M. (2006) *J. Am. Chem. Soc.* 128, 7566–7571
14. Cornilescu, G., Delaglio, F., & Bax, A. (1999) *J. Biomol. NMR* 13, 289–302
15. Brunger, A.T., Adams, P.D., Clore, G..M., Delano, W.L., Gros, P., & Grosse-Kunstleve, R.W. et al., Crystallography and NMR System (CNS) (1.1 edit.), Yale University, New Haven, CT (1997–2001)
16. Nederveen, A.J., Doreleijers, J.F., Vranken, W., Miller, Z., Spronk, C.A., & Nabuurs, S.B. et al., (2005) Proteins 59 , 662–672
17. Hooft, R.W., Vriend, G., Sander, C., & Abola, E.F. (1996) *Nature* 381, 272
18. Laskowski, R.A., Rullmannn, J.A., MacArthur, M.W., Kaptein, R., and Thornton, J.M. (1996) *J. Biomol NMR* 8, 477–486
19. Koradi, R., Billeter, M., and Wüthrich, K. (1996). *J. Mol. Graphics* 14, 51−55
20. Hubbard, S.J., and Thornton, J.M. (1993). 'NACCESS', Computer Program, Department of Biochemistry and Molecular Biology, University College London